J. Fluid Mech. (1986), *vol.* 166, *pp.* 41–56
Printed in Great Britain

Effect of opposing buoyancy on the flow in free and wall jets

By DANIEL GOLDMAN AND YOGESH JALURIA
Department of Mechanical and Aerospace Engineering,
Rutgers University, New Brunswick, New Jersey 08903

(Received 23 August 1985 and in revised form 4 November 1985)

An experimental investigation is carried out into the characteristics of the velocity and thermal fields in free and wall jets in which the buoyancy force opposes the flow. The flow configuration considered is that of a negatively buoyant two-dimensional jet discharged adjacent to a vertical surface, as well as that discharged away from the boundaries of the region. Such convective flows are frequently encountered in heat-rejection processes and in enclosure fires, where, at various locations, the buoyancy force is upward while the flow is downward, resulting in negative buoyancy. An experimental system is developed to study the downward penetration of such jets in which the buoyancy force opposes the externally induced flow. The penetration distance is measured and related to the inflow conditions, particularly the temperature and velocity at the discharge location. A steady state is simulated by allowing the fluid to flow out of the enclosure at the open top. The velocity and temperature distributions are also measured, in order to understand the basic nature of such flows. Several other effects, such as the entrainment into the flow, are also considered in this study.

1. Introduction

There are several practical circumstances where the buoyancy force is in a direction opposite to that of the flow. For example, in an enclosure fire, when the fire plume hits the ceiling, it spreads out over the ceiling and finally turns downward at the corners, see Alpert (1975) and Cooper *et al.* (1980). At this stage, the flow in the jet is downward, whereas the buoyancy force is upward, since the flow is at a temperature higher than its surroundings. Similarly, buoyant flows rising adjacent to two walls may flow along the ceiling, meet at the top and be pushed downward against the buoyancy force, because of mass conservation. This results in a negatively buoyant two-dimensional free jet. Thermal energy discharges into the ambient air-and-water medium also frequently result in negatively buoyant flows, as studied by Prahl, Ostrach & Tong (1977) and by Satyanarayana & Jaluria (1982). Therefore, it is important to study the characteristics of such negatively buoyant flows subjected to a buoyancy force acting against the direction of flow, which is driven by an externally induced pressure difference, such as that due to a blower or a fire plume.

A downward negatively buoyant flow is retarded because of the buoyancy force which acts vertically upward. This results in a decrease in the velocity of the flow, which ultimately reaches a stagnation point and then reverses direction. Therefore, the flow penetrates to a finite depth δ_p in the ambient environment before reversal occurs. The ambient fluid is entrained into the flow, resulting in a larger flow rate at the level of the jet source compared with that discharged by the negatively buoyant

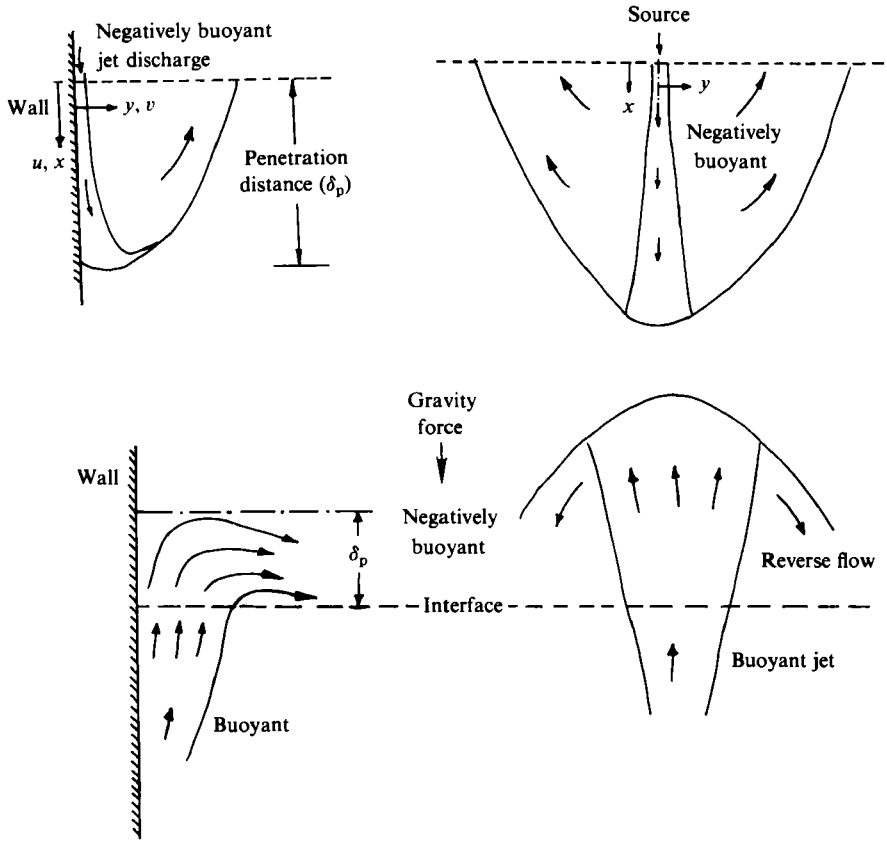

FIGURE 1. Negatively buoyant jet and wall flows.

jet $\dot{m}_{in}$. Figure 1 shows, qualitatively, the basic characteristics of negatively buoyant flows. The flow is of a mixed-convection type resulting from the interaction between the buoyancy force and the externally induced momentum input. In this figure, the interface refers to a demarcation between regions where the flow is positively and negatively buoyant.

Of particular interest in many of the practical problems mentioned above are the penetration distance δ_p and the total flow rate $\dot{m}_{out}$ at the level of the source for a two-dimensional jet, see Jaluria & Steckler (1982) and Jaluria (1984). It is also important to determine the dependence of these quantities on the inflow velocity and temperature, characterized in terms of the inlet Reynolds number Re and Grashof number Gr, defined later. This information should provide important inputs into the design and analysis of systems where such flows are encountered. Since many of these flows occur adjacent to walls, it is important to compare the results for discharge adjacent to a wall with those for discharge away from the wall.

The negatively buoyant axisymmetric jet has been studied analytically by means of an integral model and some experimental work has also been done as reported by Turner (1966) and Seban, Behnia & Abreu (1978). The results obtained for that flow indicate that the flow penetrates to a finite depth, where the vertical velocity drops to zero and flow reversal occurs, as expected. The flow spreads out horizontally as it approaches the location of flow reversal. The analysis did not consider the effect of the reverse flow on the externally driven jet flow. It considered a point-source jet

with momentum and buoyancy input, but zero mass flux at the inlet. A boundary-layer formulation was employed, with Taylor's entrainment assumption, as given by Morton, Taylor & Turner (1956) and reviewed by Turner (1979). Since the transverse velocity component is comparable with the vertical one near the region where the flow reversal occurs, a boundary-layer analysis is not expected to apply in this region. However, predictions of the penetration distance have been found to be close to the experimentally determined values, but the flow rates and the velocity and temperature distributions are not accurately predicted by analysis, as discussed by Seban *et al.* (1978).

No detailed experimental or analytical effort has been directed at two-dimensional, negatively buoyant flows, though work has been done on buoyant jets, particularly axisymmetric jets, see for instance Morton (1959), Mollendorf & Gebhart (1973) and Jaluria (1986). Of particular interest in such negatively buoyant flows, with respect to enclosure fires and heat rejection problems, are the flow rates and the penetration distances. A detailed experimental study is needed to determine these quantitatively and examine their dependence on the governing parameters in the problem. This paper presents the results obtained from a detailed experimental investigation of turbulent, two-dimensional heated air jets discharged downward. The penetration distance δ_p is measured over wide ranges of the governing parameters. Velocity and temperature profiles are also measured. The flow is visualized by means of smoke introduced into the jet, upstream of the discharge location.

It is found that the flow mainly depends on the mixed-convection parameter Gr/Re^2, which is the inverse of a Froude number, over the parametric ranges considered. Here, Gr and Re are the Grashof and Reynolds numbers respectively, as defined later. A considerable amount of mixing is found to arise near the region of flow reversal, resulting in a large entrainment of the ambient fluid into the flow. A strong reverse flow is generated, which is expected to influence the main, downward flow substantially. The basic nature of the flow is studied and related to the combined transport mechanisms resulting from the momentum and buoyancy input.

2. Experimental arrangement

Before proceeding to a description of the experimental set-up and the measurement system, the basic considerations underlying the design of the experiment shall be outlined. For this purpose, the governing equations for the flow may be considered to yield the dimensionless parameters appropriate for presenting the experimental data in generalized terms.

2.1. *Governing equations*

The governing equations for a laminar, two-dimensional negatively buoyant jet, such as a heated jet discharged downward, are (Jaluria 1982, 1986)

$$\frac{\partial u}{\partial x}+\frac{\partial v}{\partial y}=0, \tag{1}$$

$$u\frac{\partial u}{\partial x}+v\frac{\partial u}{\partial y}=\nu\frac{\partial^2 u}{\partial y^2}-g\beta(T-T_\infty), \tag{2}$$

$$u\frac{\partial T}{\partial x}+v\frac{\partial T}{\partial y}=\alpha\frac{\partial^2 T}{\partial y^2}, \tag{3}$$

where the boundary-layer approximations have been made. Fluid properties are taken as constant, except for density variation in the momentum equation for which the Boussinesq approximation is employed (Jaluria 1980). Here, x is the vertical coordinate distance measured from the exit slot, y the horizontal coordinate distance measured from the wall or the axis, see figure 1, and u, v the corresponding velocity components. Also, T denotes the local temperature, T_∞ the ambient temperature, g the magnitude of the gravitational acceleration, β the coefficient of thermal expansion of the fluid, α the thermal diffusivity and ν the kinematic viscosity.

These equations may be non-dimensionalized by employing the slot width D, the average discharge velocity of the jet U_0 and the average temperature T_0 at the slot as the characteristic length, velocity and temperature respectively. Then, the non-dimensional variables, given on the left-hand side of the following equations, are

$$X = \frac{x}{D}, \quad Y = \frac{y}{D}, \quad \theta = \frac{T-T_\infty}{T_0-T_\infty}, \quad U = \frac{u}{U_0}, \quad V = \frac{v}{U_0} \tag{4}$$

The dimensionless governing boundary-layer equations are then obtained as

$$\frac{\partial U}{\partial X} + \frac{\partial V}{\partial Y} = 0, \tag{5}$$

$$U\frac{\partial U}{\partial X} + V\frac{\partial U}{\partial Y} = \frac{1}{Re}\frac{\partial^2 U}{\partial Y^2} - \frac{Gr}{Re^2}\theta, \tag{6}$$

$$U\frac{\partial \theta}{\partial X} + V\frac{\partial \theta}{\partial Y} = \frac{1}{Re\,Pr}\frac{\partial^2 \theta}{\partial Y^2}, \tag{7}$$

where the Reynolds number Re, the Prandtl number Pr and the Grashof number Gr are defined as

$$Re = \frac{U_0 D}{\nu}, \quad Pr = \frac{\nu}{\alpha}, \quad Gr = \frac{g\beta(T_0-T_\infty)D^3}{\nu^2}. \tag{8}$$

The boundary conditions may be written as

$$\begin{aligned} &\text{at} && X = 0: && U = \theta = 1.0, && \text{for} && Y \leqslant 1.0, \\ & && && U = \theta = 0.0, && \text{for} && Y > 1.0, \\ &\text{at} && X > 0: && U \to 0, && \theta \to 0, && \text{as} && Y \to \infty, \\ & && && \frac{\partial U}{\partial Y} = \frac{\partial \theta}{\partial Y} = V = 0, && \text{at} && Y = 0. \end{aligned} \tag{9}$$

The last condition applies for a free jet. For a wall jet over an adiabatic surface, this condition may be replaced by

$$U = V = \frac{\partial \theta}{\partial Y} = 0, \quad \text{at} \quad Y = 0. \tag{10}$$

It is seen from the above formulation that the governing parameters are Re, Pr and Gr, or Gr/Re^2, which is also often written as $1/Fr$, where $Fr\,[= U_0^2/g\beta(T_0-T_\infty)D]$ is known as the discharge Froude number. A Richardson number Ri, where $Ri = g\beta(T_0-T_\infty)D/U_0^2$, may also be defined instead. The parameter Gr/Re^2 is frequently known as the mixed-convection, or buoyancy, parameter (Jaluria 1980). The equations are given for laminar flow. However, a similar treatment may be carried out for turbulent flow, employing a suitable closure model. For the eddy-

viscosity model, α is replaced by $\alpha+\epsilon_H$ and ν by $\nu+\epsilon_M$, where ϵ_H and ϵ_M are eddy diffusivity and viscosity respectively, as outlined by Madni & Pletcher (1977). Though additional parameters arise due to the turbulence modelling employed, the basic governing parameters are still the same as those for laminar flow. If Boussinesq approximations are not employed, the Froude number may be written as $Fr = U_0^2/(gD\Delta\rho/\rho_0)$, where $\Delta\rho = \rho_\infty - \rho_0$, ρ_∞ being the ambient fluid density and ρ_0 the density at the jet discharge. Similarly, integral models, with an entrainment assumption, also lead to Re, Pr and Gr/Re^2, or Fr^{-1}, as the basic governing parameters, see Jaluria (1980) and Satyanarayana & Jaluria (1982). Therefore, these parameters, particularly Re and Gr/Re^2, are chosen for the presentation of the results, since Pr is essentially constant over the experimental range.

2.2. *Experimental system*

Figure 2 shows a sketch of the experimental arrangement. A blower sends ambient air, over a wide range of flow rates, through a copper tube which is about 5 cm in diameter and 1 m in length. The copper tube is kept hot by means of electrically heated strip heaters wrapped around it. A diffuser at the end of the tube allows the heated air to emerge as a two-dimensional jet, whose width may be varied. Several diffuser designs were considered to ensure uniform flow at the exit. Measurements indicated that fairly uniform velocity and temperature are obtained at the discharge. An insulation jacket reduces the energy loss from the copper tube to the environment. The air temperature at the jet outlet is monitored by means of a thermocouple and the flow rate is measured by a flow meter, positioned in the flow upstream of the blower. It was ascertained that wide ranges of the Reynolds and Grashof number, Re and Gr respectively, can be obtained, as mentioned earlier. These ranges can easily be increased by replacing the blower by one of larger capacity and by adding an additional strip heater around the copper tube. Most of the measurements presented here have been taken for Re ranging from around 1000 to 5000 and for Gr from zero to 10^6. The width of the slot is varied from about 1 to 7 cm and its length is 30 cm, so that the aspect ratio varies from 30 to about 5. The resulting flow field was ascertained to be closely two-dimensional by measurement of temperature and velocity across the third dimension.

The heated, two-dimensional, air jet is discharged downward in a glass tank about 1.5 m high and 0.4×0.3 m in cross-section. The bottom is kept open to allow the discharged fluid to entrain ambient air or to flow out at a relatively small velocity level, resulting in a negligible effect of the opening on the negatively buoyant flows under study. The jet can be located near the centre of the top or adjacent to the wall in order to study various flow configurations. The top, as well as the sidewalls, can be moved or completely removed to study the effect of openings on the flow. If the top is removed, the negatively buoyant flow buoys back out of the enclosure, resulting ultimately in a steady flow. If the top is closed, an upper layer of heated fluid builds up and the interface with the lower, cooler layer gradually drops in height resulting in a transient situation. For the measurements reported here, the far wall of the enclosure, see figure 2, was removed so as to avoid any constraint on the entrainment due to this wall.

The thermal field is measured using copper–constantan thermocouples and the velocity distribution by a constant-temperature hot-wire anemometer. A probe assembly is used with a traversing arrangement to position the thermocouples and the hot-wire at any desired location in the flow. A data acquisition system, which employs an analog-to-digital converter with an Apple personal computer, is used for

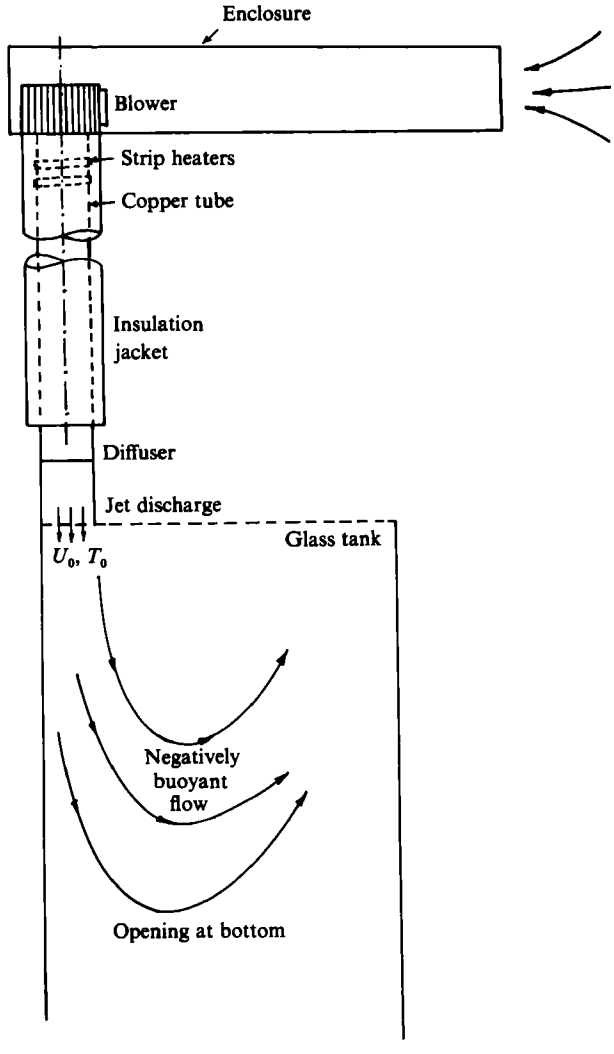

FIGURE 2. Experimental arrangement.

storing the data for subsequent analysis on a Prime computer system. The flow is visualized by means of smoke generated by the evaporation of kerosene oil as it flows through an electrically heated steel tube. A dense white smoke is obtained, whose concentration in the flow can be made small to ensure a negligible disturbance to the flow. The smoke is introduced into the flow upstream of the diffuser so that it heats up with the air and exits at the same local temperature as the jet. The smoke can also be injected at various transverse locations in the jet to study local trends.

A DISA hot-wire anemometer is employed for velocity measurements. The hot-wire is calibrated by measuring the frequency of the vortices behind a long cylinder, as described by Roshko (1953). A long thin wire is stretched across the circular tube through which air flows at room temperature. The frequency in the wake allows the determination of the air velocity across the cylinder. This information is used for both the calibration of the hot-wire and the computation of the mass flow rate, by measuring the velocity profile across the tube. The thermocouples were calibrated

using a constant-temperature bath. The velocity and temperature distributions are measured and information on penetration and entrainment is extracted from these. Flow visualization is employed to study the nature of the flow qualitatively and to guide the choice of locations for temperature and velocity measurements.

3. Experimental results and discussion

3.1. *Flow visualization*

A detailed study of the thermal and flow fields was undertaken. The flow was visualized with smoke, as described above, and the initial experiments were directed at studying the basic nature of the flow. In all the results discussed here, the top cover of the tank was removed so that a steady state could eventually be attained. Photographs showing the typical movement of smoke introduced into a steady flow are shown in figure 3. Figure 3(*a*) shows the enclosure before the onset of the flow and figure 3(*d*) shows the steady state obtained by the flow. It was found that the flow develops very rapidly from the inflowing jet of figure 3(*b*), through flow reversals of figure 3(*c*), to a steady, penetrative flow with a fairly constant depth of penetration. The flow was found to spread out horizontally and generate a considerable amount of mixing in the upper part of the enclosure. This mixing is expected to give rise to substantial entrainment of fluid from the bottom, as confirmed by later experimentation. The penetration depth was found to depend strongly on the inflow parameters, as expected and as seen quantitatively below. Because of the large horizontal spread of the flow, the far wall of the enclosure was removed and the sidewalls were extended to obtain a two-dimensional flow in an extensive environment.

3.2. *Flow penetration*

The penetration distance δ_p was quantified by defining it as the vertical distance from the jet inflow to the location where the local temperature excess, $T-T_\infty$, has dropped to 1% of the inlet excess, T_0-T_∞. This is similar to the definition of boundary-layer thickness (Jaluria 1980). The measured value was also compared with the value estimated from visualization studies and a fairly good agreement was obtained.

The dependence of the penetration distance δ_p, normalized by the slot width D, on the Grashof and Reynolds numbers is shown in figures 4 and 5. It is interesting to note that the jet penetrates to the bottom of the enclosure for small Gr, as expected, and attains an essentially constant penetration distance at large Gr. Penetration is also seen to increase with Re, as expected, and to again approach a constant value at large Re. This indicates a dominant effect of Gr in determining penetration and the approach to a minimum penetration distance of around $10D$ at high values of Gr, for the given range of Re.

The variation of δ_p with the mixed-convection parameter Gr/Re^2 is shown in figures 6 and 7 for a wall jet, as well as for a free jet. The data shown correspond to several values of Gr and Re, obtained by varying U_0, T_0 and D. It is evident from these figures that the downward penetration distance is very well correlated in terms of Gr/Re^2, over the ranges of Gr and Re investigated, since a single curve fits the data for different Gr and Re. Thus only a weak additional dependence on Re is indicated. Similar trends have been observed for turbulent free jets, see Turner (1979). The asymptotic behaviour at large and small Gr is also seen in these figures. Thus, over the range of parameters investigated, the penetration-depth results may be expressed in terms of only Gr/Re^2, or Fr^{-1}, the inverse of the Froude number. Obviously, at

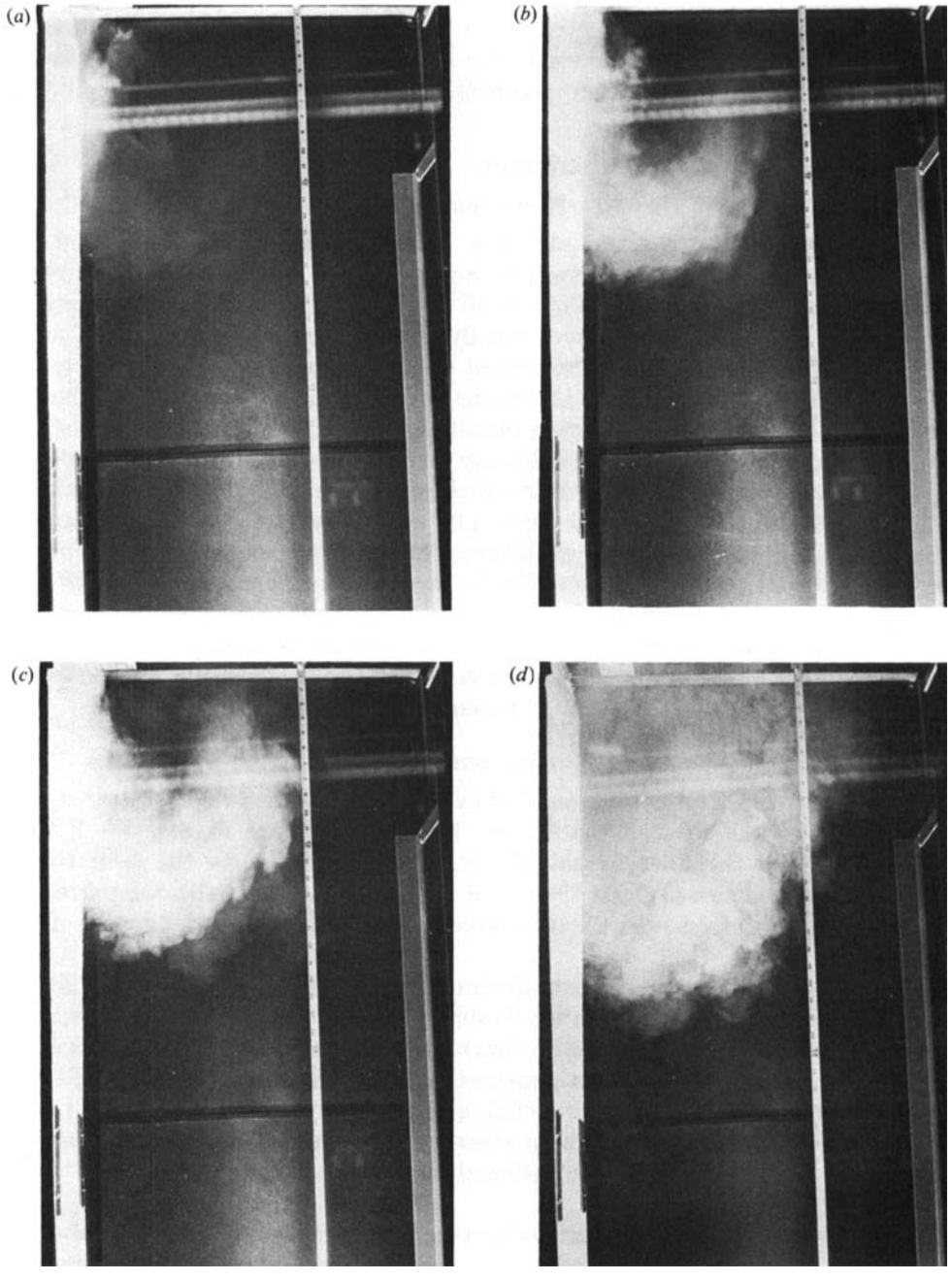

FIGURE 3. Photographs of (*a*) the experimental arrangement and (*b*), (*c*) and (*d*) three stages in the movement of smoke introduced into a steady two-dimensional negatively buoyant jet.

small Gr, the additional dependence on Re is expected to appear, as at large Gr the dependence on Gr would appear (Jaluria 1980, 1985). The downward penetration of the wall jet was found, from the data obtained, to be less than that of the free jet, mainly because of the wall shear. However, the difference between the two was quite small, as seen from the figures. The wall was insulated in all these results and the

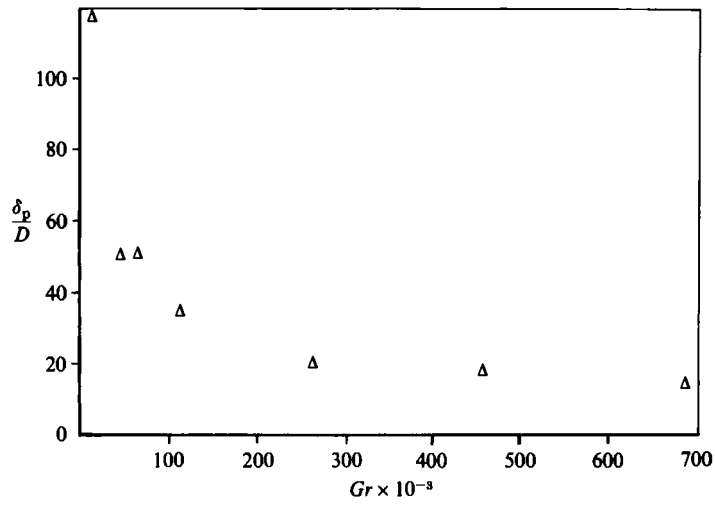

FIGURE 4. Downward penetration distance δ_p as a function of the Grashof number Gr, at $Re = 4670$. ($T_0 - T_\infty = 37.9$ °C, D varied.)

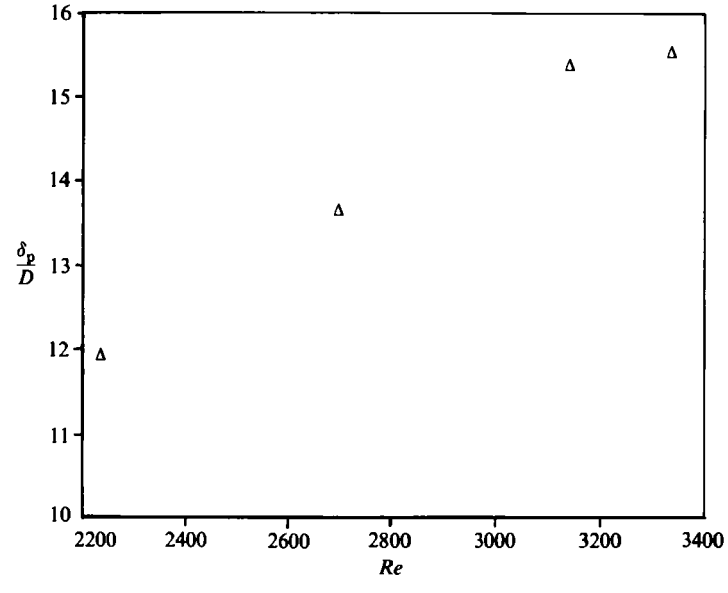

FIGURE 5. Downward penetration distance δ_p as a function of the Reynolds number Re, at $Gr = 3.15 \times 10^5$. ($D = 4.0$ cm, $T_0 - T_\infty = 52.3$ °C, U_0 varied.)

trends may change if substantial heat transfer occurs at the wall.The penetration-distance results, given in figures 4–7, were obtained by measuring the temperature distributions in the flow and determining the location where the temperature excess is 1 % of the excess at the inlet. Therefore, each data point represents a fairly elaborate measurement of the temperature distributions in the flow.

An attempt was made to correlate the data presented in figures 6 and 7 by plotting

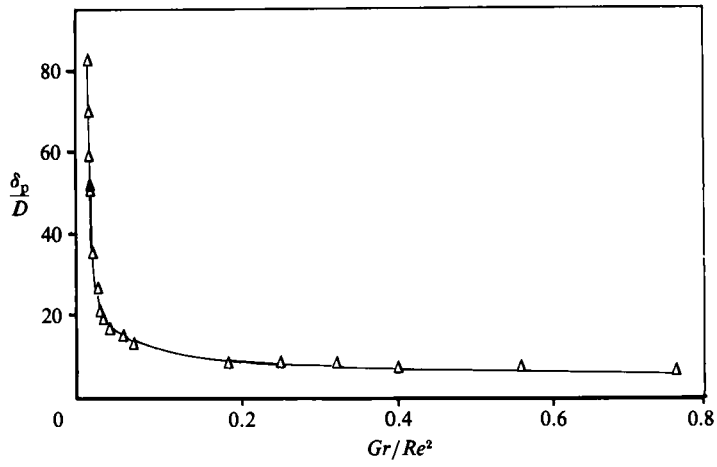

FIGURE 6. Variation of the downward penetration distance δ_p with the mixed-convection parameter Gr/Re^2, for a wall jet: ——, equation (11).

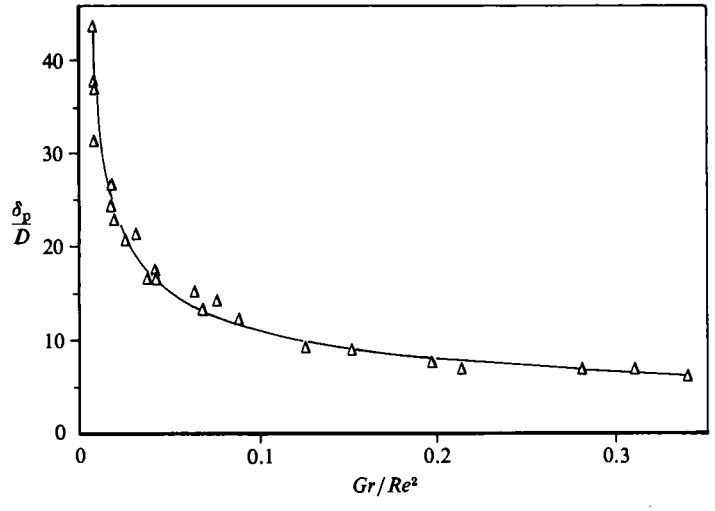

FIGURE 7. Variation of the downward penetration distance δ_p with the mixed convection parameter Gr/Re^2, for a free jet away from the wall: ——, equation (12).

the results on a log–log graph, obtaining the dependence of the penetration distance δ_p/D on Gr/Re^2, over the range $0 \lesssim Gr/Re^2 \lesssim 1.0$, as

wall Jet:
$$\frac{\delta_p}{D} = 4.424\left(\frac{Gr}{Re^2}\right)^{-0.389}, \tag{11}$$

free Jet:
$$\frac{\delta_p}{D} = 3.959\left(\frac{Gr}{Re^2}\right)^{-0.440}. \tag{12}$$

These equations were found to represent the data very closely over the range of Gr/Re^2 investigated, as seen in figures 6 and 7. Obviously, these equations do not apply for

$Gr/Re^2 \to \infty$, since a zero penetration distance is physically unrealistic. Also, our results indicate the approach to a constant value of δ_p as $Gr/Re^2 \to \infty$. However, very large values of this parameter were not of interest in this study and were not investigated and so equations (11) and (12) may be taken to apply for $0 \lesssim Gr/Re^2 \lesssim 1.0$.

It must be noted that D is a suitable characteristic dimension if the penetration distance δ_p is not too large compared with D. If the flow penetrates to large distances, of order $100D$, the effect of D on the flow would be expected to be small at large x. The input variables would then be the momentum and buoyancy at the discharge and, if these are held constant, a variation in D would not be expected to significantly affect the results. In this case, a theoretical penetration distance δ_{th} may be defined by balancing the inflowing kinetic energy by the work done against buoyancy as $\frac{1}{2}\rho_0 U_0^2 = g\Delta\rho\delta_{th}$, to give $\delta_{th}/D = \frac{1}{2}Fr = \frac{1}{2}Re^2/Gr$. The $\frac{1}{2}$ in these equations may be dropped, since this is only an order-of-magnitude analysis, to yield $\delta_{th}/D \approx O(Fr)$. Therefore, if $\delta_p \gg D$, we may employ δ_{th}, given by $\delta_{th} = DFr = \rho_0 U_0^2/g\Delta\rho$, as the characteristic dimension, see Prahl *et al.* (1977) and Jaluria (1980). However, in the flow region near the discharge location, the slot width is the appropriate characteristic dimension. Since our interest lies in this region, the results are presented in terms of the non-dimensionalization given by (4).

These results on the penetration distance are of considerable value in the mathematical modelling of enclosure fires. At the initial stages of fire growth, the downward penetration of the wall flow driven by the fire plume is relevant to the establishment of the upper layer. Also, the penetration of the wall flows, following the establishment of the two zones, is important in considerations of energy and mass balance. Similarly, thermal discharges into the environment often give rise to such negatively buoyant flows. The penetration distance is also a very important aspect in this case.

3.3. *Velocity and temperature fields*

Extensive measurements of the temperature and velocity distributions were taken in order to quantify the basic characteristics of the flow, such as entrainment into the flow, horizontal spread of the flow region, penetration distance and heat transfer at the wall. A few typical profiles are presented here. Figure 8 shows the velocity and temperature profiles across the tank for a given set of experimental conditions, at various values of the vertical distance x from the jet discharge location. As mentioned earlier, two fluid streams arise downstream, downward and upward.

It is seen from the temperature data that the demarcation between the two is not very sharp because of thermal diffusion. At large x, near the location where the flow turns around, a large scatter in the data is observed, mainly because of the large amount of mixing there. The temperature level in the downward flow gradually decreases as the distance from the slot is increased. This is expected since temperature decays away from the source owing to entrainment of ambient air. It is also seen that the temperature gradient at the wall is not zero, indicating that the surface is not adiabatic. The surface is obviously not perfectly insulated, and some energy transport does occur there. It is very hard to obtain a perfectly insulated surface in air, because of its low conductivity. The thermal conductivity of the wall material is 4–5 times that of air. Also, in practice, energy exchange between the fluid and the wall would generally occur. The heat-transfer rate and the surface-temperature variation may be computed from this data. It may also be noted that the wall adjacent to the

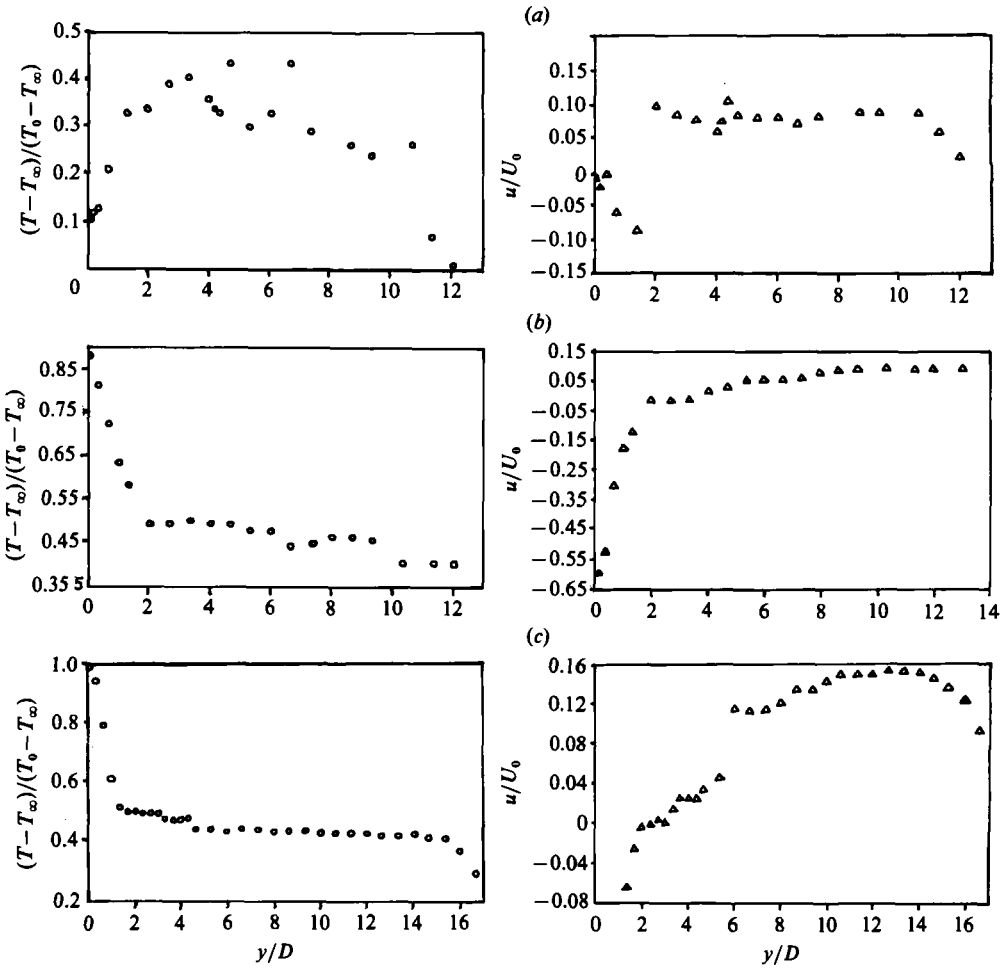

FIGURE 8. Temperature and velocity profiles across the enclosure, for a wall jet, at $Gr/Re^2 = 0.00678$; (a) $x/D = 30.50$; (b) 4.24; (c) 0.1 ($U_0 = 2.57$ m/s, $T_0 - T_\infty = 35.7$ °C, $D = 3.0$ cm).

discharge becomes heated due to conduction, while the jet temperature decreases due to entrainment of ambient fluid, resulting in heat transfer to the fluid at small x. At large distances from the source, the fluid is still hot and loses energy to the surface.

Another interesting feature observed from these results is the almost uniform temperature and velocity over much of the reverse, upward flow. This effect is not surprising when one considers the tremendous mixing generated by the flow and the consequent horizontal spreading out of the flow region. Therefore, these results indicate that the downward flow, which is very localized near the source, results in a very large region of reverse flow further downstream. For these inlet conditions, the velocity and temperature are also found to be fairly uniform in the upward flow. The temperature level in the reverse flow shows a slight decrease, due to continued entrainment, as the flow moves up. The velocity level in this reverse flow increases upward due to buoyancy. It is interesting to note that the uniform temperature distribution at the discharge is rapidly replaced by a non-uniform one in only a short downstream distance. This is obviously a consequence of the much smaller temperature levels in the upward flow, see figure 8(c). Also, as expected, a region of small velocity

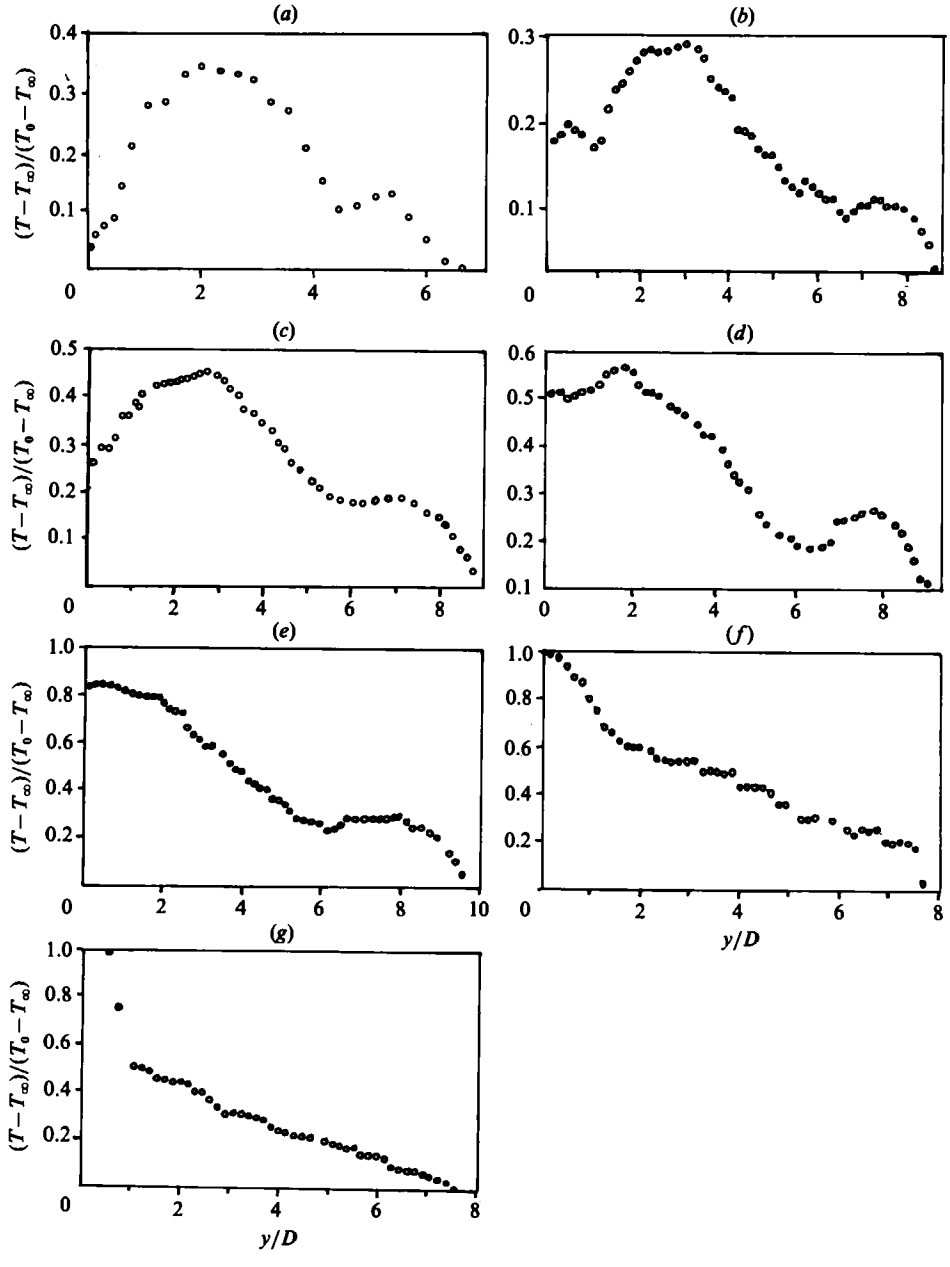

FIGURE 9. Temperature profiles across the enclosure, for a wall jet, at $Gr/Re^2 = 0.0483$; (*a*) $x/D = 13.70$; (*b*) 11.72; (*c*) 9.77; (*d*) 7.69; (*e*) 5.86; (*f*) 4.89; (*g*) 0.05 ($U_0 = 1.1$ m/s, $T_0 - T_\infty = 31.2$ °C, $D = 6.5$ cm).

levels arises between the downward flow at the discharge and the upward flow out of the enclosure.

Several other similar measurements of the velocity and temperature profiles were taken. Figure 9 shows the detailed temperature distributions in the flow, at essentially the same value of *Re* but at a much larger *Gr*, this difference being due to the change in the slot width. The result is a decrease in the jet velocity at the inlet and an increase

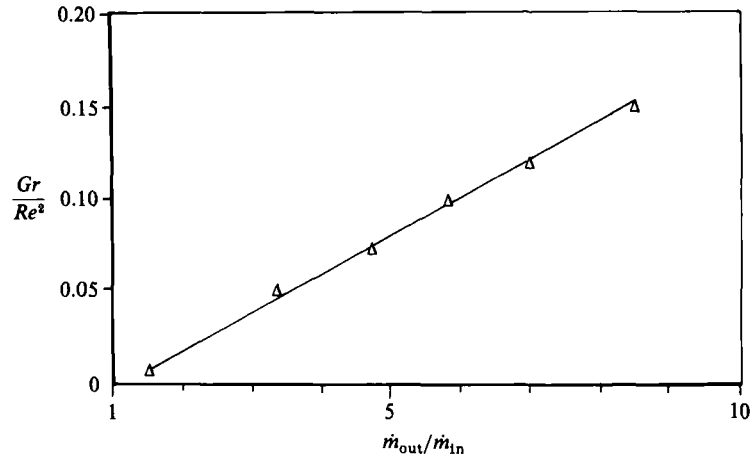

FIGURE 10. Variation of the net flow out of the enclosure $\dot{m}_{out}$, normalized by the jet discharge flow rate $\dot{m}_{in}$, as a function of the mixed convection parameter Gr/Re^2: ——, equation (13).

in the buoyancy effect. The jet penetrates to a shorter dimensionless vertical distance δ_p/D. It is also interesting to note the demarcation between the downward and upward streams of fluid, as seen earlier in figure 3. A stronger buoyancy force tends to generate a strong upward flow, resulting in the hump seen in the distributions of figure 9. The general trends, in terms of temperature decay downstream and flow spread, are similar to those seen in figure 8. Again, as explained above, energy transfer occurs from the surface to the flow at small x and from the fluid to the surface at large x. This is obviously a consequence of conduction transport into the wall which heats up the region near the jet inlet. The surface is insulated, though obviously not perfectly adiabatic, and the jet exchanges about 10–15 % of its energy input with the surface.

The net flow out of the enclosure $\dot{m}_{out}$ at the level of the jet discharge, was computed and compared with the inflow $\dot{m}_{in}$. It was found that the flow rate out the enclosure can be as high as about ten times that discharged into it by the jet. Figure 10 shows the variation of the ratio $\dot{m}_{out}/\dot{m}_{in}$ as a function of the mixed-convection parameter Gr/Re^2. It is interesting to note that the ratio increases almost linearly with Gr/Re^2, attaining a value of 8.5 at $Gr/Re^2 = 0.16$. A higher value of Gr/Re^2 implies a larger buoyancy effect, which results in a shorter penetration distance and a stronger reverse flow, which in turn leads to a larger ambient-fluid entrainment. The mass-flow ratio $\dot{m}_{out}/\dot{m}_{in}$ was found to be well-correlated by the following equation, over the range $0.01 \lesssim Gr/Re^2 \lesssim 0.15$:

$$\frac{\dot{m}_{out}}{\dot{m}_{in}} = 1.074 + 49.03\left(\frac{Gr}{Re^2}\right). \tag{13}$$

This result is also of considerable value in the mathematical modelling of such flows, since it allows an estimation of the total entrainment as a function of the inlet conditions. An entrainment coefficient can also be estimated from this data, as a function of Gr/Re^2, for use in integral models. Similar entrainment values have been observed by Zukoski (1984) for other buoyancy-driven flows in enclosure fires.

4. Conclusions

A detailed experimental study has been carried out to study the basic characteristics of negatively buoyant wall and free jets. The effect of opposing buoyancy on the externally induced jet flow is a very important consideration in many problems of practical interest, such as enclosure fires and thermal discharge into the environment. Two-dimensional, turbulent flows are considered and the velocity and thermal fields, resulting from the interaction of the opposing buoyancy force with the input momentum, are investigated. The penetration distance δ_p is measured and is found to be largely dependent on the mixed-convection parameter Gr/Re^2, which may also be represented as the inverse of a discharge Froude number Fr. A steady state is simulated and the net entrainment into the flow is determined. With increasing buoyancy effects, as indicated by an increase in Gr/Re^2, the flow penetration decreases and a stronger reverse flow, in the direction of the buoyancy force, arises. The entrainment into the flow is found to increase with Gr/Re^2, as a consequence of the increased reverse flow at larger Gr/Re^2.

As expected, two fluid streams are generated, one driven by the externally introduced momentum, with opposing buoyancy, and the other by the buoyancy force. The two streams are found to be somewhat distinct at larger Gr/Re^2 because of the dominant buoyancy effect. However, at lower values of Gr/Re^2, the reverse flow is weaker and diffusion effects lead to a fairly gradual variation of velocity and temperature across the two streams. The wall jet is retarded because of the shear of the wall. Also, the heat transfer at the wall is found to be an important effect. An interesting aspect that is observed in this study is the attainment of a minimum penetration distance as the Grashof number is increased to large values. The region where the externally induced flow becomes stationary and the reverse flow takes over is found to be very disturbed owing to the large changes in the flow occurring at this location. This is found to result in an extensive horizontal spreading out of the flow and in a substantial amount of ambient-fluid entrainment. Several other interesting aspects are observed in this flow and related to the basic mechanisms that govern the transport processes.

This research was carried out with support from the Center for Fire Research of the National Bureau of Standards, United States Department of Commerce, Grant No. NB83NADA4047, under the technical management of Dr Leonard Y. Cooper.

REFERENCES

ALPERT, R. L. 1975 Turbulent ceiling-jet induced by large scale fires. *Combust. Sci. Tech.* **11**, 197.

COOPER, L. Y., HARKLEROAD, M., QUINTIERE, J. & RINKINEN, W. 1982 An experimental study of upper hot layer stratification in full-scale multiroom fire scenarios. *Trans. ASME* C: *J. Heat Transfer* **104**, 741.

JALURIA, Y. 1980 *Natural Convection Heat and Mass Transfer*. Pergamon.

JALURIA, Y. 1982 Buoyant plane jets in thermally stratified media. *ASME Paper No.* 82-WA/HT-57.

JALURIA, Y. 1984 Buoyancy-induced wall flow due to fire in a room. *Natl Bur. Stand., Rep.* NBSIR-84-2841.

JALURIA, Y. 1986 Hydrodynamics of laminar buoyant jets. In *Encyclopedia of Fluid Mechanics* (ed. J. P. Cheremisinoff), vol. 2, chap. 12, Gulf (to appear).

JALURIA, Y. & STECKLER, K. D. 1982 Wall flow due to fire in a room. In *Proc. Fall Tech. Meeting, East. Sect. Combust. Inst., Atlantic City, NJ*, Paper No. 47.

MADNI, I. K. & PLETCHER, R. H. 1977 Buoyancy jets discharging nonvertically into a uniform quiescent ambient – a finite-difference analysis and turbulence modeling. *Trans. ASME* C: *J. Heat Transfer* **99**, 641.

MOLLENDORF, J. C. & GEBHART, B. 1973 An experimental and numerical study of the viscous stability of a round laminar jet with and without thermal buoyancy for symmetric and asymmetric disturbances. *J. Fluid Mech.* **61**, 367.

MORTON, B. R. 1959 Forced Plumes. *J. Fluid Mech.* **5**, 151.

MORTON, B. R., TAYLOR, G. I. & TURNER, J. S. 1956 Turbulent gravitational convection from maintained and instantaneous sources. *Proc. R. Soc. Lond.* A**234**, 1.

PRAHL, J., OSTRACH, S. & TONG, T. 1977 The discharge of a submerged buoyant jet into a stratified environment. In *Proc. Waste Heat Mgt. Util. Conf., Miami Beach, Florida, 3, VIII-B* p. 135.

ROSHKO, A. 1953 On the development of turbulent wakes from vortex streets. *NACA Tech. Rep.* 1191.

SATYANARAYANA, S. & JALURIA, Y. 1982 A study of laminar buoyant jets discharged at an inclination to the vertical buoyancy force. *Intl J. Heat Mass Transfer* **25**, 1569.

SEBAN, R. A., BEHNIA, M. M. & ABREU, J. E. 1978 Temperatures in a heated jet discharged downward. *Intl J. Heat Mass Transfer* **21**, 1453.

TURNER, J. S. 1966 Jets and plumes with negative or reversing buoyancy. *J. Fluid Mech.* **26**, 779.

TURNER, J. S. 1979 Buoyancy Effects in Fluids. Cambridge University Press.

ZUKOSKI, E. 1984 Internal flows and combustion in two-layer room fire models. *Ann. Conf. Fire Res., NBS, Gaithersburg, MD.*